MIMO communications within the HF band using compact antenna arrays

S. D. Gunashekar,[1] E. M. Warrington,[1] S. M. Feeney,[2] S. Salous,[2] and N. M. Abbasi[1]

Received 12 April 2010; revised 7 July 2010; accepted 19 August 2010; published 3 December 2010.

[1] Measurements have been made over a 255 km radio path between Durham and Leicester in the UK in order to investigate the potential applicability of multiple input multiple output (MIMO) techniques to communications within the HF band. This paper describes the results from experiments in which compact heterogeneous antenna arrays have been employed. The results of these experiments indicate that traditional spaced HF antenna arrays can be replaced by compact, active, heterogeneous arrays in order to achieve the required levels of decorrelation between the various antenna elements. An example case study is also presented which highlights the importance of the variable nature of the ionosphere in the context of HF-MIMO radio links.

Citation: Gunashekar, S. D., E. M. Warrington, S. M. Feeney, S. Salous, and N. M. Abbasi (2010), MIMO communications within the HF band using compact antenna arrays, *Radio Sci.*, *45*, RS6013, doi:10.1029/2010RS004416.

1. Introduction

[2] For several years now, multiple input multiple output (MIMO) technology has been applied to the field of wireless communications in order to attain higher data rates. The majority of developments in this area have been directed toward wireless applications operating in the VHF, UHF and SHF bands [*Foschini*, 1996; *Foschini and Gans*, 1998; *Shiu et al.*, 2000; *Wallace and Jensen*, 2002; *Lim et al.*, 2007; *Razavi-Ghods and Salous*, 2009], with very little research conducted in the lower frequency bands.

[3] In order to investigate the feasibility of utilizing MIMO techniques within the High Frequency (HF) band to provide enhanced data rates, several experimental campaigns have been performed over a dedicated, approximately north-south (bearing is equal to 173°) radio path of length 255 km between Durham and Bruntingthorpe (near Leicester) in the UK (see Figure 1). Preliminary investigations reported by *Warrington et al.* [2008] and *Gunashekar et al.* [2008, 2009a, 2009b] demonstrated that conventional spaced antenna arrays can provide useful levels of interelement decorrelation, although at times significant spacing on the order of several tens of meters may be required (an important requirement of a successful MIMO system are sufficiently low values of cross-correlation values between the antenna elements comprising the arrays at both ends of the radio link). Additionally, marked antenna orientation-dependent fading effects have been observed in some of the earlier experiments.

[4] This paper reports on experiments in which compact, heterogeneous antenna arrays (discussed in section 2) have been utilized at both ends of MIMO links with the aim of reducing the space requirements. The focus will be on the use of two arrays based on active electronics that have been developed for receiver applications to provide broadband nontuned operation with electrically small receiving elements. Additionally, preliminary observations from experiments that have utilized a compact transmitting antenna array will be discussed.

2. Types of Antenna Arrays

[5] As opposed to homogeneous antenna arrays that are composed of the same types of antenna elements, all oriented in the same direction (see, for example, the circularly disposed antenna arrays discussed by *Gething* [1991] and the homogeneous circular array reported by *Erhel et al.* [2004]), heterogeneous antenna arrays can either have (1) different types of antenna elements [e.g., *Marie et al.*, 2000; *Oger et al.*, 2006], or (2) the same types of antenna elements with different orientations [e.g., *Erhel et al.*, 2004; *Gunashekar et al.*, 2009a]. The principle of heterogeneity can be exploited in the design

[1]Radio Systems Research Group, Department of Engineering, University of Leicester, Leicester, UK.
[2]Centre for Communication Systems, School of Engineering, University of Durham, Durham, UK.

0048-6604/10/2010RS004416

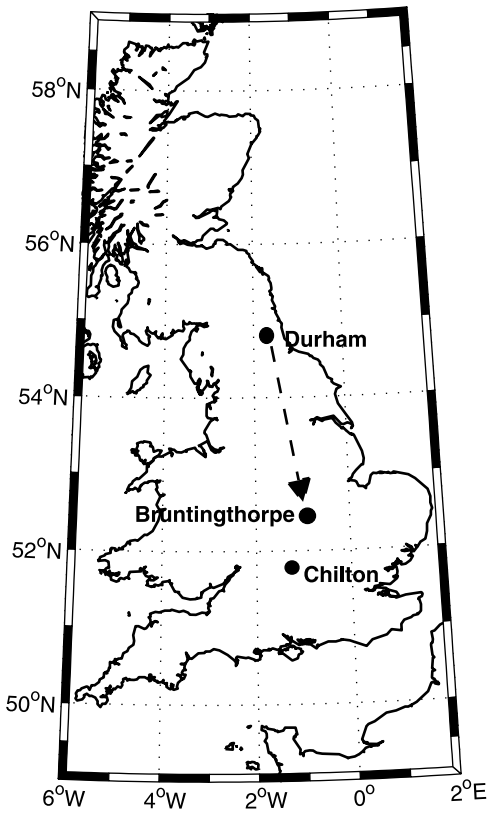

Figure 1. Map depicting locations of the transmitter and receiver sites, and the Chilton ionosonde station.

of compact, colocated antenna arrays by means of which decorrelation between the antenna elements may be obtained at a single location removing the need for large antenna spacings. Previously, these antenna arrays have been used in direction finding applications [*Marie et al.*, 2000; *Erhel et al.*, 2004] as well as at the receiving ends of HF-SIMO links to improve the transmission of images [*Perrine et al.*, 2004; *Erhel et al.*, 2005].

2.1. Description of Colocated, Heterogeneous Receiving Antenna Arrays Used in the HF-MIMO Experiments

[6] This section provides a brief description of the design of two candidate heterogeneous receiving antenna arrays for HF-MIMO applications. By employing active electronics, physically compact configurations have been realized by using electrically small (relative to the wavelength) receiving elements to sense either the electrical or magnetic component of the incoming wave. The constructions of the antennas allow operation across a wide range of frequencies in order to accommodate variations in the ionospheric propagation conditions. A more detailed discussion of the design and technical specifications of these antenna arrays can be found in the work of *Feeney et al.* [2009].

2.1.1. "X-Y-Z" Loop Array

[7] The structure consists of three electrostatically screened active loops (each approximately 1 m square) arranged orthogonally, i.e., two vertical loops and a horizontal loop (see Figure 2). The electrically small loops effectively act as magnetic field sense elements or H field antennas. During the experiments, the array was oriented so that the vertical elements were in the N-S (pointing in the general direction of Durham) and E-W directions.

2.1.2. Ground Symmetric Loop Array

[8] This array is based on the design of an antenna configuration (called the "Giselle" antenna array) developed by *Massie et al.* [2004]. The structure (see Figure 3) comprises three active screened magnetic square loops (each approximately 1 m square) that are inclined to one another such that the antennas have the same geometry with respect to the ground (i.e., they are ground symmetric). As a result of the inclinations, the tops of each of the three loops form the sides of an equilateral triangle in the horizontal plane. Similarly, the lower ends of the

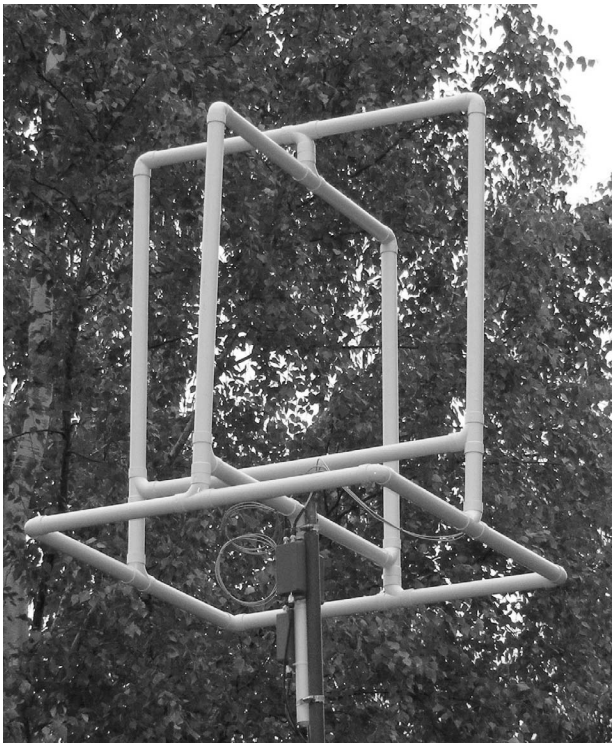

Figure 2. "X-Y-Z" loop array: example of a compact HF receiving antenna array composed of three mutually orthogonal square loop antennas.

Figure 3. Ground symmetric loop (GSL) array: example of a compact HF receiving antenna array composed of three square loop antennas inclined at angles so that all have the same geometry with respect to the ground.

three loops form another equilateral triangle in the horizontal plane (this triangle is inverted relative to the triangle at the top of the array).

2.2. Description of a Colocated, Heterogeneous Transmitting Antenna Array Used in the HF-MIMO Experiments

[9] This section provides a brief description of a compact, heterogeneous HF antenna array that has been recently developed for transmitting applications. *Feeney et al.* [2009] provide further details about the technical specifications of this array.

[10] This array (see Figure 4) is composed of a pair of colocated, resonant magnetic loop antennas that are arranged orthogonally in the vertical plane. Each loop forms a 1.5 m by 1.5 m octagon and a 2.5 m long aluminum box section has been used to support the antenna array during the experimental campaigns.

3. Performance of the Heterogeneous Arrays

3.1. Experiment Utilizing the Heterogeneous Receiving Antenna Arrays

[11] In this section, observations and results are presented from HF-MIMO measurements in which both the "X-Y-Z" array and the ground symmetric loop (GSL) array were simultaneously employed. The results from these arrays are compared with those of the crossed inverted "V" wire array that in earlier measurements exhibited consistently low levels of decorrelation between the two perpendicularly oriented wires [*Gunashekar et al.*,

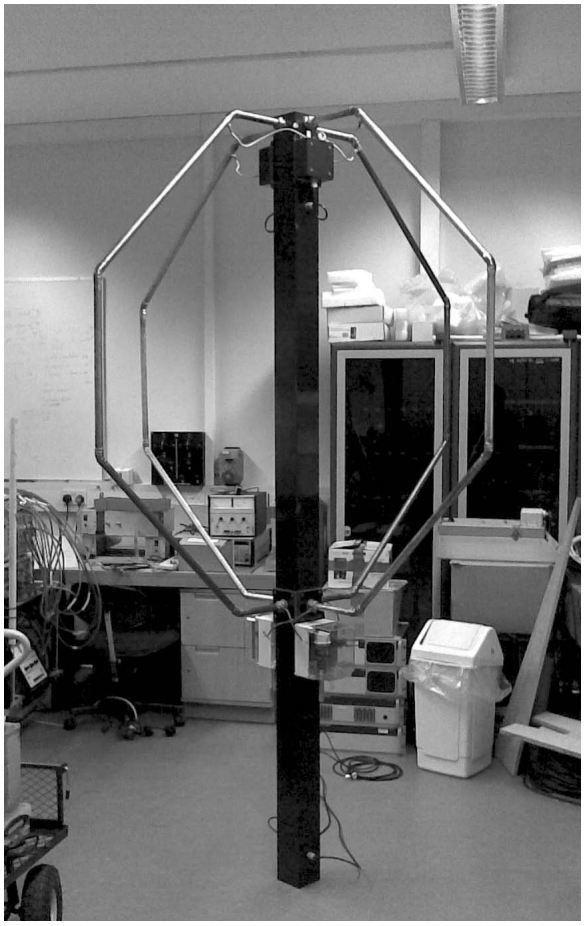

Figure 4. Compact transmitting loop array consisting of two mutually perpendicular and vertically oriented octagonal loop antennas.

2008, 2009a, 2009b; *Warrington et al.*, 2008]. Note that a commonly used correlation coefficient value that is often cited as a threshold below which signals are generally considered to be independent of each other is 0.7 [*Waldschmidt et al.*, 2002; *Mtumbuka et al.*, 2005]. Higher values are often regarded as acceptable and *Loyka* [2001] reports that for a 10-element uniform linear array, the MIMO channel capacity does not degrade significantly until the interelement correlation coefficient exceeds a value as high as 0.9.

3.1.1. Experimental Arrangement

[12] A 2 × 8 MIMO campaign was conducted on 19 June 2009. At the transmitter, a pair of end-fed, resistively terminated, and orthogonally oriented (N-S and E-W) inverted "V" wire antennas was used. The N-S arm of the array (TX-2) that was pointing in the general direction of the receiving site (bearing is equal to 173°), and the E-W arm of the array (TX-1) were supported by the same mast, and were "crossed" at a common point located approximately 8 m above ground level. Each inverted "V" arm composed of approximately 34 m of stranded stainless steel wire. The nominal transmission frequency was 5.255 MHz (TX-1: 5.255020 MHz; TX-2: 5.255030 MHz). As discussed by *Gunashekar et al.* [2009b], the frequency offsets were necessary as a means of identifying the different transmit signals.

[13] For the receiving array, eight antennas were deployed: an end-fed, crossed inverted "V" wire antenna array identical to that used at the transmitter (RX-1: N-S crossed inverted "V" wire; RX-2: E-W crossed inverted "V" wire), the ground symmetric loop array (RX-3: GSL loop–1; RX-4: GSL loop–2; RX-5: GSL loop–3) and the "X-Y-Z" active loop array (RX-6: N-S vertical loop; RX-7: E-W vertical loop; RX-8: horizontal loop). The three arrays were arranged in a line in the east-west direction with the following separations between the masts supporting each of the arrays: Crossed inverted "V" wire array–GSL array: 32.2 m; GSL array–"X-Y-Z" array: 37.2 m.

3.1.2. Results and Discussion

[14] The experiment was carried out for approximately 45 min (between 1135 UT and 1220 UT) with both TX-1 and TX-2 simultaneously transmitting. 34 one minute data files were collected at each of the receiving antennas.

[15] Vertical ionograms were obtained from the Chilton ionosonde located approximately 215 km from the midpoint of the Durham-Bruntingthorpe path at a bearing of about 180° (see Figure 1). The vertical ionograms, when overlaid with suitable transmission curves, indicated the existence of multiple ionospheric propagation modes, providing the multipath propagation required for successful MIMO operation. This was confirmed by the resulting amplitude plots from the collected data that depicted deep signal fading on all the receiving antennas for both transmissions.

[16] As noted in section 1, a key requirement for successfully implementing a MIMO system is the need for sufficiently low levels of correlation between the various antennas at each end of the link. The occurrence frequency histograms of the correlation coefficients (of the 60 s amplitude records) between the loop antennas comprising the "X-Y-Z" array and GSL array are depicted in Figures 5 and 6, respectively. The correlation coefficient values, corresponding to both transmissions, TX-1 (E-W arm of the inverted "V" wire array) and TX-2 (N-S arm of the inverted "V" wire array) have been presented for all the data collected during the measurement campaign.

[17] In general, both compact arrays yield useful levels of decorrelation. With reference to the "X-Y-Z" array (Figure 5), in particular for the two pairs involving the N-S oriented vertical loop, the majority of the correlation coefficient values lie below 0.7. Specifically, for the N-S and E-W loops, approximately 60% and 85% of the correlation coefficient values are less than 0.7 for TX-1 and TX-2, respectively, while for the N-S and horizontal loops, the corresponding values of correlation coefficient that do not exceed 0.7 are 82% (for TX-1) and 94% (TX-2). For the GSL array pair comprising loops 2 and 3, 76% and 91% of the correlation coefficient data do not exceed 0.7 for transmissions TX-1 and TX-2, respectively.

[18] For comparison, the histograms of the correlation coefficients between the N-S and E-W inverted "V" wire receiving antennas (for both TX-1 and TX-2) are shown in Figure 7. Majority of the correlation coefficient values lie in the range 0.6–0.9 indicating that under the prevailing ionospheric conditions, the compact, heterogeneous antenna arrays may replace the considerably larger inverted "V" wire array. The mean values of the correlation coefficients for the various pairs of receiving antennas have been listed in Table 1 for both transmissions, TX-1 and TX-2. Over the complete measurement period, the receiving pairs involving the compact antenna elements are almost always more decorrelated (sometimes by a significant margin) than the N-S and E-W arms of the long wire antenna array, indicating the suitability of the "X-Y-Z" and GSL arrays to replace larger antenna arrays at the receiving ends of HF-MIMO links.

[19] In addition to the decorrelation results, it was also noted that in general, the output amplitude from the horizontal loop of the "X-Y-Z" array was lower than that recovered from the vertical N-S and E-W loops. *Massie et al.* [2004] report that for a similar construction of an "X-Y-Z" antenna array, the horizontal loop appears to have a different phase center compared to the two vertically oriented loops. The GSL array, on the other hand,

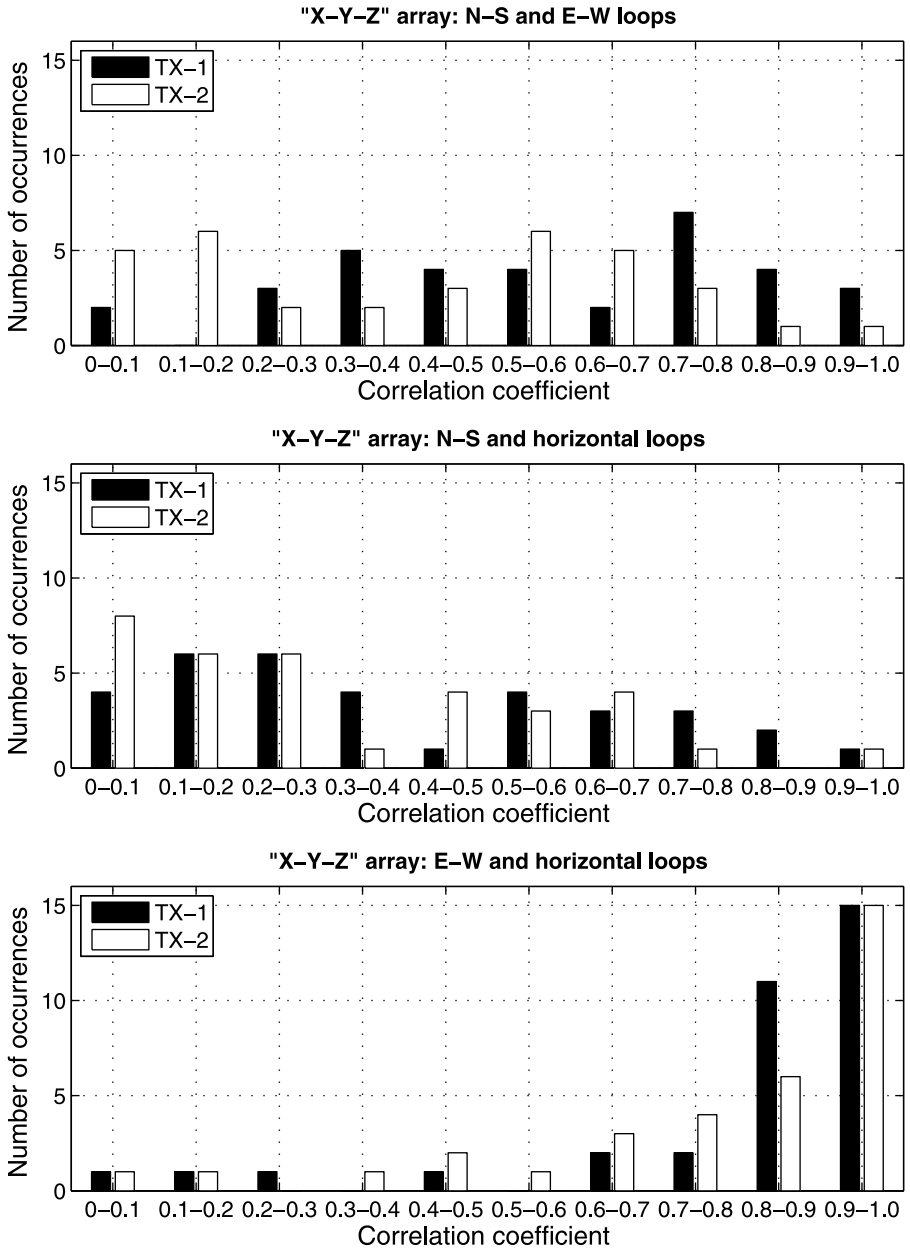

Figure 5. The occurrence frequency histograms of the magnitudes of correlation coefficients (of 60 s amplitude records) between the following three pairs of colocated, perpendicular loop antennas comprising the "X-Y-Z" receiving array, for both transmissions (TX-1: E-W arm of inverted "V" wire array; TX-2: N-S arm of inverted "V" wire array): (top) N-S and E-W loops; (middle) N-S and horizontal loops; (bottom) E-W and horizontal loops. The 2 × 8 MIMO campaign was conducted between Durham and Bruntingthorpe on 19 June 2009 (nominal transmission frequency: 5.255 MHz; 34 one minute data files were analyzed).

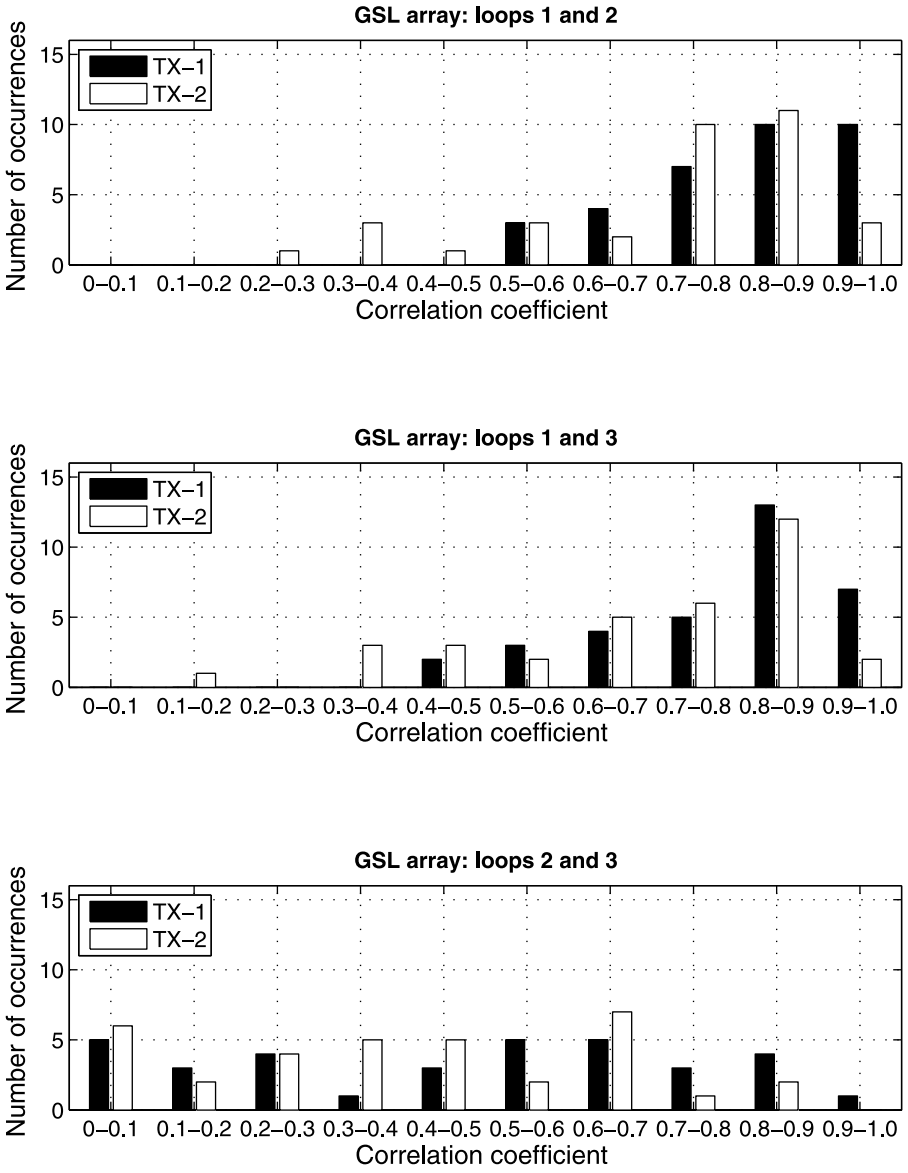

Figure 6. The occurrence frequency histograms of the magnitudes of correlation coefficients (of 60 s amplitude records) between the following three pairs of loop antennas comprising the GSL receiving array, for both transmissions (TX-1: E-W arm of inverted "V" wire array; TX-2: N-S arm of inverted "V" wire array): (top) loops 1 and 2; (middle) loops 1 and 3; (bottom) loops 2 and 3. The 2 × 8 MIMO campaign was conducted between Durham and Bruntingthorpe on 19 June 2009 (nominal transmission frequency: 5.255 MHz; 34 one minute data files were analyzed).

demonstrates a more uniform output signal level on all three loops, in addition to exhibiting useful levels of interelement decorrelation when sufficient numbers of ionospheric modes are present.

3.2. Experiment Utilizing the Dual Loop Transmitting Array

[20] On 25 March 2009, a 4 × 8 MIMO campaign was conducted in order to examine the performance of the

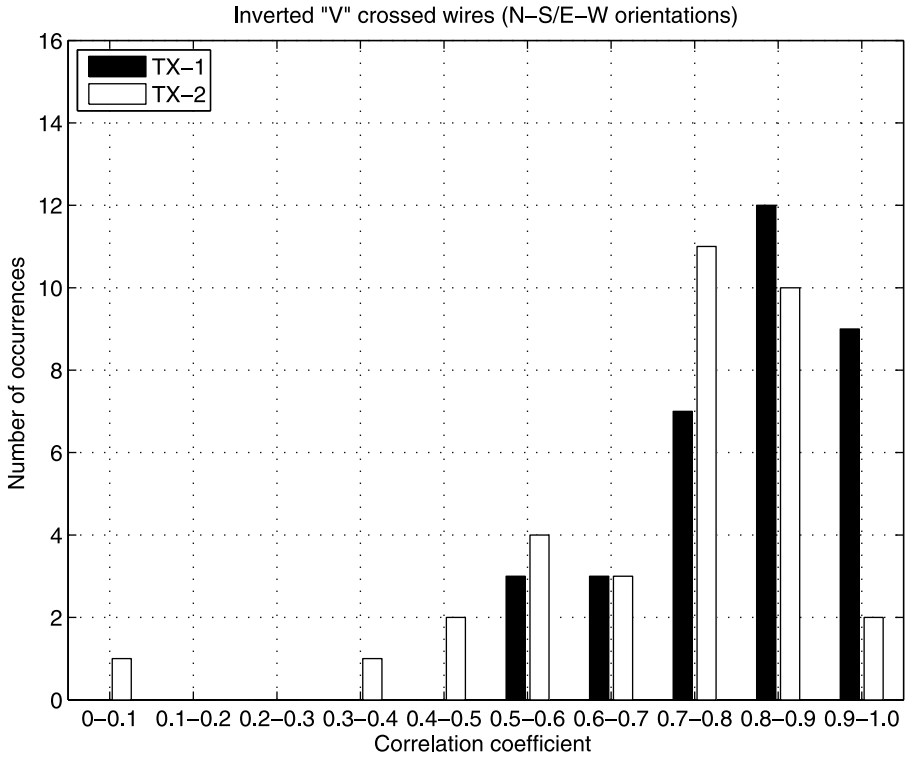

Figure 7. The occurrence frequency histograms of the magnitudes of correlation coefficients (of 60 s amplitude records) between the N-S and E-W arms of the receiving crossed inverted "V" wire antenna array, for both transmissions (TX-1: E-W arm of inverted "V" wire array; TX-2: N-S arm of inverted "V" wire array). The 2 × 8 MIMO campaign was conducted between Durham and Bruntingthorpe on 19 June 2009 (nominal transmission frequency: 5.255 MHz; 34 one minute data files were analyzed).

compact, transmitting loop array consisting of the two colocated, perpendicular (N-S and E-W) octagonal loop antennas (described in section 2.2).

3.2.1. Experimental Arrangement

[21] With the intention of providing an appropriate means of comparison, a pair of end-fed, crossed inverted "V" wire antennas (TX-1: N-S inverted "V" wire; TX-2: E-W inverted wire) was utilized at the transmitter, in addition to the dual loop array (TX-3: N-S octagonal loop; TX-4: E-W octagonal loop). The crossed inverted "V" wire array was identical to the one described in section 3.1.1. The nominal transmission frequency used in this campaign was 4.455 MHz (TX-1: 4.455020 MHz; TX-2: 4.455030 MHz; TX-3: 4.455010 MHz; TX-4: 4.455040 MHz), and the output power was approximately 50 W per antenna.

[22] At the receiver, the following antenna arrays were employed: an end-fed, crossed inverted "V" wire antenna array (RX-1: N-S crossed inverted "V" wire; RX-2: E-W crossed inverted "V" wire), a crossed dipole and vertical monopole active array (RX-3: N-S crossed dipole; RX-4:

Table 1. Mean Values of the Amplitude Correlation Coefficients Between Various Pairs of Receiving Antennas for Both Transmissions During a 2 × 8 HF-MIMO Campaign Conducted Between Durham and Bruntingthorpe on 19 June 2009[a]

Receiving Antenna Pairs Being Correlated	Transmitter	Mean Correlation Coefficient
"X-Y-Z" array: N-S	TX-1	0.58
and E-W loops	TX-2	0.42
"X-Y-Z" array: N-S	TX-1	0.40
and horizontal loops	TX-2	0.33
"X-Y-Z" array: E-W	TX-1	0.81
and horizontal loops	TX-2	0.77
GSL array: loops 1 and 2	TX-1	0.81
	TX-2	0.72
GSL array: loops 1 and 3	TX-1	0.79
	TX-2	0.70
GSL array: loops 2 and 3	TX-1	0.48
	TX-2	0.39
Colocated N-S and E-W inverted	TX-1	0.82
"V" long wire antennas	TX-2	0.72

[a]TX-1: E-W arm of crossed inverted "V" wire array; TX-2: N-S arm of crossed inverted "V" wire array. Nominal transmission frequency: 5.255 MHz; 34 one minute data files were analyzed.

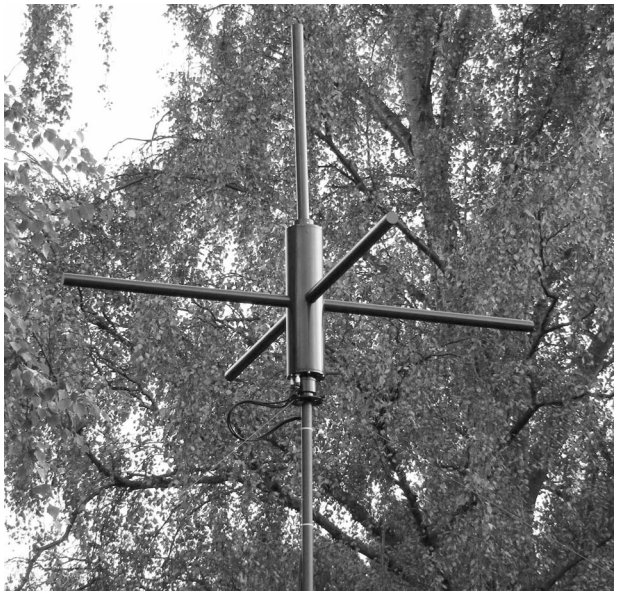

Figure 8. Example of a compact HF receiving antenna array comprising a pair of orthogonal dipoles in the horizontal plane and a single vertical monopole.

E-W crossed dipole; RX-5: vertical monopole; see Figure 8), and the "X-Y-Z" active array (RX-6: N-S vertical loop; RX-7: E-W vertical loop; RX-8: horizontal loop). The three arrays were aligned in the east-west direction with the following separations: Crossed inverted "V" wire array–"X-Y-Z" array: 57 m; "X-Y-Z" array-crossed dipole and vertical monopole array: 21 m. The experiment was undertaken between 1348 UT and 1456 UT during which 45 one minute data files were collected for each receiving antenna.

3.2.2. Results and Discussion

[23] The occurrence frequency histograms of the amplitude correlation coefficients between the N-S and E-W oriented transmit loop antennas at two receiving antennas are presented in Figure 9 (receiving antenna: N-S inverted "V" wire) and Figure 10 (receiving antenna: E-W loop of the "X-Y-Z" array), respectively. For comparison, Figures 9 and 10 also contain the histograms of the correlation coefficients between the transmitting N-S and E-W oriented inverted "V" wire antennas. In Figures 9 and 10, the distribution of correlation coefficients between the transmitting loops is comparable to that obtained with the significantly larger inverted "V" wire array. This behavior was noted at all eight receiving antennas indicating the suitability of the compact transmit array to replace physically larger antennas.

[24] To reinforce this observation, Table 2 contains a list of the mean amplitude correlation coefficients for both pairs of transmitting antennas at the eight receiving antennas for the complete measurement period (i.e., for all 45 one minute data files). Not only are all the mean correlation coefficient values less than 0.8, the compact transmitting loop array is observed to always outperform the crossed inverted "V" wire array in terms of the level of decorrelation between the respective perpendicular elements.

4. Significance of the Number of Ionospheric Modes

[25] This section presents an illustrative example that provides direct evidence of the dependence of the levels of correlation between antenna elements (and hence MIMO capacity) on the number of multipath components present in the ionosphere.

4.1. Experimental Arrangement

[26] A 2 × 8 MIMO link was established on 29 January 2009. At the transmitter, two colocated (supported by the same mast) orthogonal end-fed inverted "V" long wire antennas were used to simultaneously transmit continuous wave signals at a nominal frequency of 5.255 MHz (TX-1: N-S crossed inverted "V" wire pointing in the general direction of Bruntingthorpe; TX-2: E-W crossed inverted "V" wire). The nominal transmit power on each antenna was approximately 50 W. These signals were received, between 1248 UT and 1429 UT, at the following heterogeneous antenna arrays (69 one minute data files were collected): (1) End-fed, crossed inverted "V" wire antenna array similar to the one used at the transmitter (RX-1: N-S crossed inverted "V" wire pointing in the general direction of Durham; RX-2: E-W crossed inverted "V" wire) between 1248 UT and 1348 UT. (2) Colocated, active crossed dipole antennas (RX-1: N-S crossed dipole pointing in the general direction of Durham; RX-2: E-W crossed dipole) between 1354 UT and 1429 UT. A photograph of this antenna array is shown in Figure 8 (the vertical monopole antenna was not utilized in this experiment). (3) Colocated, active ground symmetric loop array (RX-3: GSL loop–1; RX-4: GSL loop–2; RX-5: GSL loop–3) between 1248 UT and 1429 UT (Figure 3). (4) Colocated, active "X-Y-Z" loop array (RX-6: N-S vertical loop pointing in the general direction of Durham; RX-7: E-W vertical loop: RX-8: horizontal loop) between 1248 UT and 1429 UT (Figure 2).

[27] The GSL array, "X-Y-Z" array and crossed dipole array were arranged in the east-west direction with the following separations between the central masts supporting each of the arrays: GSL array–"X-Y-Z" array: 64.6 m; "X-Y-Z" array–crossed dipole array: 20.6 m. The central mast of the resistively terminated, crossed inverted "V" wire array was erected approximately 18 m southwest of the GSL array. In section 4.2, the pairs of

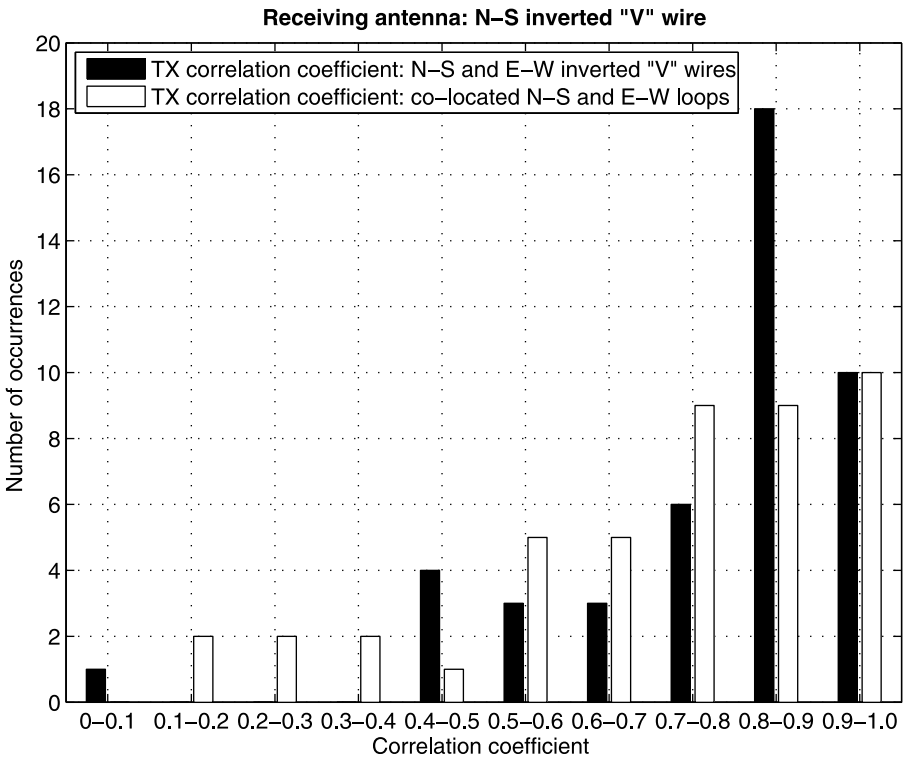

Figure 9. The occurrence frequency histograms of the magnitudes of correlation coefficients (of 60 s amplitude records) between the following two pairs of transmitting antennas at the N-S arm of the inverted "V" receiving wire array: (1) N-S and E-W arms of the inverted "V" long wire array (black data); (2) colocated N-S and E-W transmitting loops (white data). The 4 × 8 MIMO campaign was conducted between Durham and Bruntingthorpe on 25 March 2009 (nominal transmission frequency: 4.455 MHz; 45 one minute data files were analyzed).

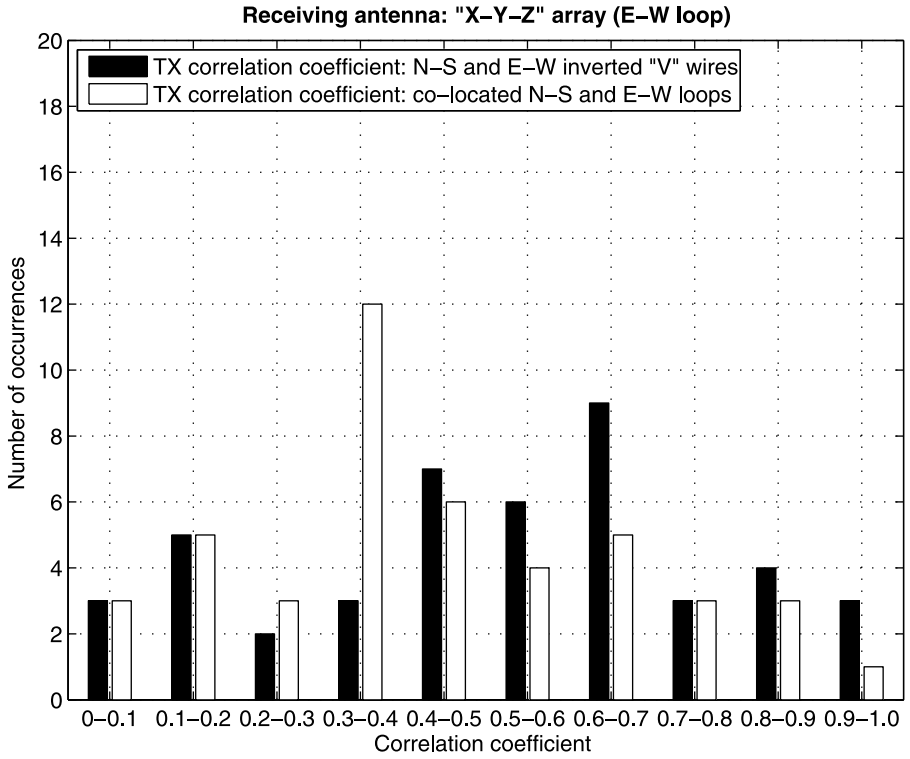

Figure 10. The occurrence frequency histograms of the magnitudes of correlation coefficients (of 60 s amplitude records) between the following two pairs of transmitting antennas at the E-W oriented loop of the "X-Y-Z" receiving array: (1) N-S and E-W arms of the inverted "V" long wire array (black data); (2) colocated N-S and E-W transmitting loops (white data). The 4 × 8 MIMO campaign was conducted between Durham and Bruntingthorpe on 25 March 2009 (nominal transmission frequency: 4.455 MHz; 45 one minute data files were analyzed).

Table 2. Mean Values (45 One Minute Data Files) of the Amplitude Correlation Coefficients Between the Colocated N-S and E-W Oriented Transmitting Loop Antennas and the Colocated N-S and E-W Oriented Inverted "V" Long Wire Antennas at Each of the Receiving Antennas for a 4 × 8 HF-MIMO Campaign Conducted Between Durham and Bruntingthorpe on 25 March 2009[a]

Receiving Antenna	Mean Correlation Coefficient Between Colocated N-S and E-W Transmitting Loop Antennas	Mean Correlation Coefficient Between Colocated N-S and E-W Transmitting Inverted "V" Long Wire Antennas
RX-1	0.71	0.77
RX-2	0.69	0.76
RX-3	0.68	0.78
RX-4	0.39	0.48
RX-5	0.53	0.66
RX-6	0.66	0.77
RX-7	0.45	0.52
RX-8	0.33	0.42

[a]RX-1: N-S arm of crossed inverted "V" long wire array; RX-2: E-W arm of crossed inverted "V" long wire array; RX-3: N-S crossed dipole; RX-4: E-W crossed dipole; RX-5: vertical monopole; RX-6: N-S vertical loop of "X-Y-Z" array; RX-7: E-W vertical loop of "X-Y-Z" array; RX-8: horizontal loop of "X-Y-Z" array.

crossed inverted "V" wires and crossed dipoles at the receiver are together referred to as the "crossed antennas." To determine the ionospheric conditions during the measurement period, transmission curves were superimposed on vertical ionograms obtained from the Chilton ionosonde (location shown in Figure 1).

4.2. Results and Discussion

[28] The number of ionospheric modes identified for the duration of the measurement campaign has been plotted in Figure 11a. Vertical ionograms at Chilton were available every 10 min and although these only give an indication of the modes likely to be present, and not the exact number of components actually present at a given time, they are nevertheless very helpful in providing general information about the state of the ionosphere. The corresponding magnitudes of correlation coefficients (of 60 s amplitude records) between various pairs of receiving antennas (indicated by the different shapes) for each transmission (indicated by the white and gray data for TX-1 and TX-2, respectively) are displayed in Figure 11b. These have been termed as "RX correlation coefficients." Similarly, for the complete measurement period, the magnitudes of correlation coefficients (of 60 s amplitude records) between the two transmitting antennas at each of the eight receiving antenna have been plotted in Figure 11c. These have been termed as "TX correlation coefficients." Figure 11d depicts the capacity estimations for various MIMO configurations (2 × 2, 2 × 3, 2 × 4, 2 × 5) for the successive data acquisitions at Bruntingthorpe (69 one minute data files), evaluated for an SNR of 30 dB, which was the approximate SNR observed in the measured data.

[29] Two distinct regions can be identified in all four plots: (1) between 1248 UT and 1304 UT, henceforth called period A, and (2) between 1304 UT and 1429 UT, henceforth called period B. During period A, approximately five ionospheric modes were identified from the vertical ionograms, while during period B, only two ionospheric modes were present for majority of the time. To illustrate the change in the state of the ionosphere over the duration of the experimental campaign, two example ionograms corresponding to periods A and B have been presented in Figures 12 and 13, respectively. The existence of a greater number of propagation paths through the ionosphere during period A has a direct bearing on the corresponding interelement correlation coefficients observed at the transmitter and receiver arrays: the values of both the TX and RX correlation coefficients are significantly lower for period A than they are for period B. Specifically, for the RX correlation coefficients, majority of the values are below 0.4 and never exceed 0.8 during period A. During period B, however, the correlation coefficients for all the receiving antenna pairs (and for both transmissions TX-1 and TX-2) almost always exceed 0.8. Additionally, during period A, it is observed that, in general, the RX correlation coefficients corresponding to the GSL array are lower than that of the "X-Y-Z" array.

[30] In the same way, the TX correlation coefficients at all the receiving antennas are considerably lower during period A (never exceeding 0.8) than during period B. The high levels of decorrelation between the different antenna elements at both ends of the link during period A consequently results in higher estimated capacities for the different MIMO configurations (Figure 11d). Not only are there slight improvements in the estimated MIMO capacities as the number of receiving antennas is increased, there is also a reduction in the channel capacities from period A (approximately five ionospheric modes) to period B (approximately two ionospheric modes).

[31] Finally, as an example, Figure 14 presents plots of amplitude against time for a period of approximately 60 s commencing at 1254:59 UT (i.e., during period A) for each of the three loops comprising the GSL array. Deep amplitude fading is observed, consistent with the existence of multiple propagation components, and the fades corresponding to both CW signals occur at different times on all three antennas (which subsequently results in the low values of RX correlation coefficient). Furthermore, at each receiving antenna, the times at which the fades occur for the two signals, TX-1 and TX-2, are dissimilar, which results in the low values of TX correlation coefficient. This behavior was noted at the other receiving antennas as well and for all the data files acquired during period A. A typical example of measurements obtained during period B is shown in

Figure 11. Observations and results obtained during a 2 × 8 HF-MIMO measurement campaign conducted between Durham and Bruntingthorpe on 29 January 2009 between 1248 UT and 1429 UT (nominal transmission frequency: 5.255 MHz; 69 one minute data files were analyzed). (a) Number of ionospheric modes identified for the radio path; (b) magnitudes of the correlation coefficients (of 60 s amplitude records) between various receiving antennas for each of the two transmissions (TX-1: N-S arm of crossed inverted "V" long wire array; TX-2: E-W arm of crossed inverted "V" long wire array); (c) magnitudes of the correlation coefficients (of 60 s amplitude records) between the two transmitting antennas at each of the eight receiving antennas; (d) capacity estimations for various MIMO configurations (2 × 2, 2 × 3, 2 × 4, 2 × 5).

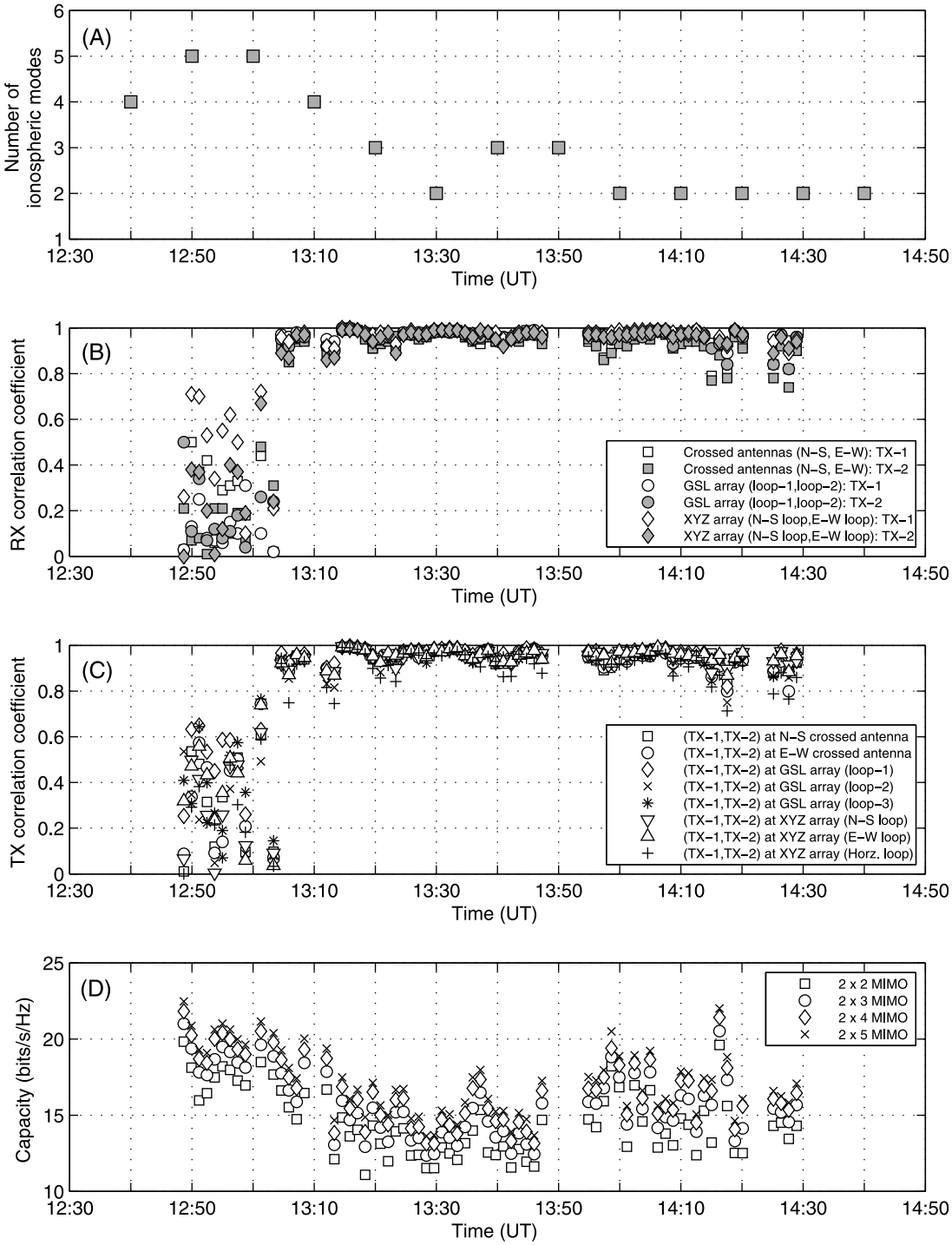
(A)
Number of ionospheric modes
Time (UT)
(B)
RX correlation coefficient
Crossed antennas (N–S, E–W): TX–1
Crossed antennas (N–S, E–W): TX–2
GSL array (loop–1,loop–2): TX–1
GSL array (loop–1,loop–2): TX–2
XYZ array (N–S loop,E–W loop): TX–1
XYZ array (N–S loop,E–W loop): TX–2
Time (UT)
(C)
TX correlation coefficient
(TX–1,TX–2) at N–S crossed antenna
(TX–1,TX–2) at E–W crossed antenna
(TX–1,TX–2) at GSL array (loop–1)
(TX–1,TX–2) at GSL array (loop–2)
(TX–1,TX–2) at GSL array (loop–3)
(TX–1,TX–2) at XYZ array (N–S loop)
(TX–1,TX–2) at XYZ array (E–W loop)
(TX–1,TX–2) at XYZ array (Horz. loop)
Time (UT)
(D)
Capacity (bits/s/Hz)
2 x 2 MIMO
2 x 3 MIMO
2 x 4 MIMO
2 x 5 MIMO
Time (UT)

Figure 11

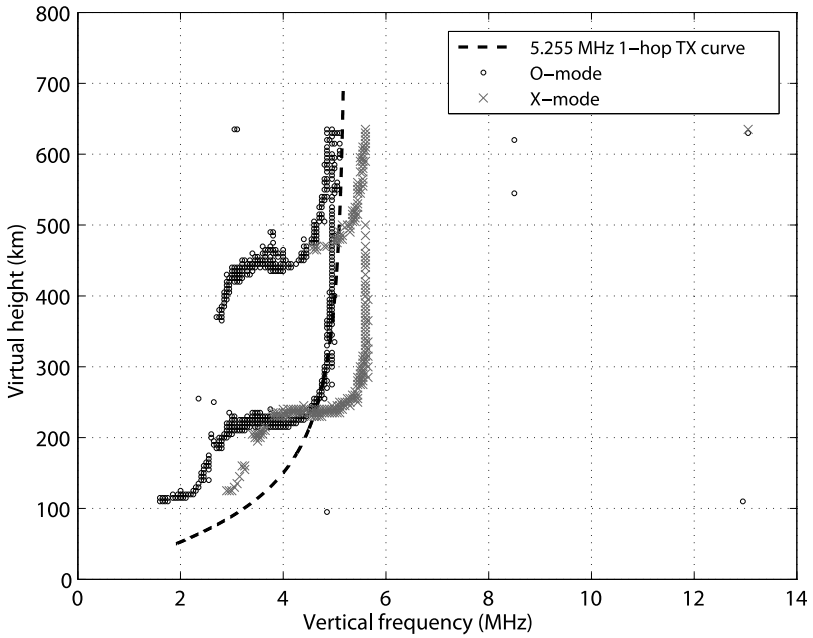

Figure 12. Vertical ionogram observed at the Chilton ionosonde station superimposed by a transmission curve (5.255 MHz) for the Durham-Bruntingthorpe path at 1250 UT on 29 January 2009.

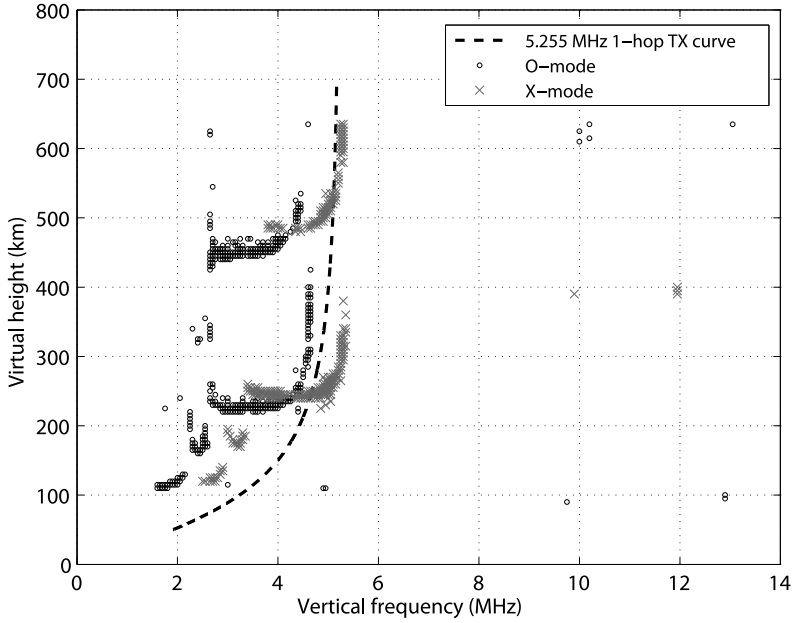

Figure 13. Vertical ionogram observed at the Chilton ionosonde station superimposed by a transmission curve (5.255 MHz) for the Durham-Bruntingthorpe path at 1420 UT on 29 January 2009.

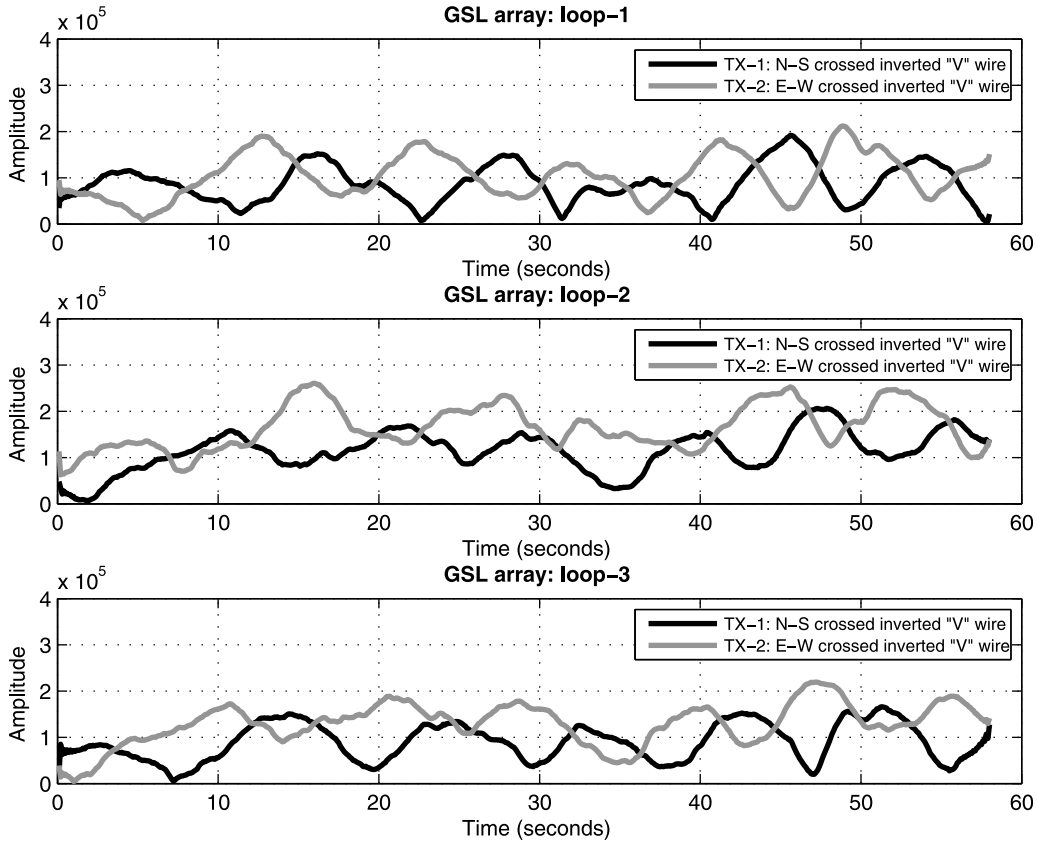

Figure 14. Amplitude patterns (in linear units) observed for a period of approximately 60 s at 1254:59 UT on 29 January 2009 on the three loops comprising the GSL array during a 2 × 8 HF-MIMO measurement campaign conducted between Durham and Bruntingthorpe. Two CW signals (offset from each other by 10 Hz) were transmitted from Durham using the crossed inverted "V" wire antenna array.

Figure 15. Figure 15 depicts the amplitude patterns observed for a period of approximately 1 min at 1346:00 UT on the three loops comprising the GSL array. In general, compared with data collected during period A, significantly less variations in signal amplitude are observed that is indicative of a reduction in the number of ionospheric modes during period B. Moreover, the fades occur at approximately the same times for both transmit signals (resulting in high TX correlation coefficients) and across all the receiving antennas (resulting in high RX correlation coefficients).

5. Concluding Remarks

[32] Current data transmission rates within the HF radio band are lower than desired by the end users and technological developments are required to overcome the limitations. MIMO techniques have the potential of increasing the channel capacity of radio systems provided suitably decorrelated paths exist between the multiple transmitter and receiver antenna elements. Previous MIMO research has focused predominantly on wireless communications within the VHF, UHF and SHF bands, and MIMO systems have not been widely investigated in the HF band for long-range communications.

[33] This paper focuses on the use of different types of compact, heterogeneous antenna arrays at both the transmitting and receiving ends of a 255 km HF-MIMO link between Durham and Bruntingthorpe in the UK. The arrays deployed in multiple experimental campaigns have demonstrated successful operation at frequencies around 5 MHz. Results have indicated that, given the presence of multiple ionospheric propagation modes, physically large HF arrays such as traditional spaced antenna arrays and inverted "V" long wire antennas, can be replaced by compact, heterogeneous arrays. This has the consequence

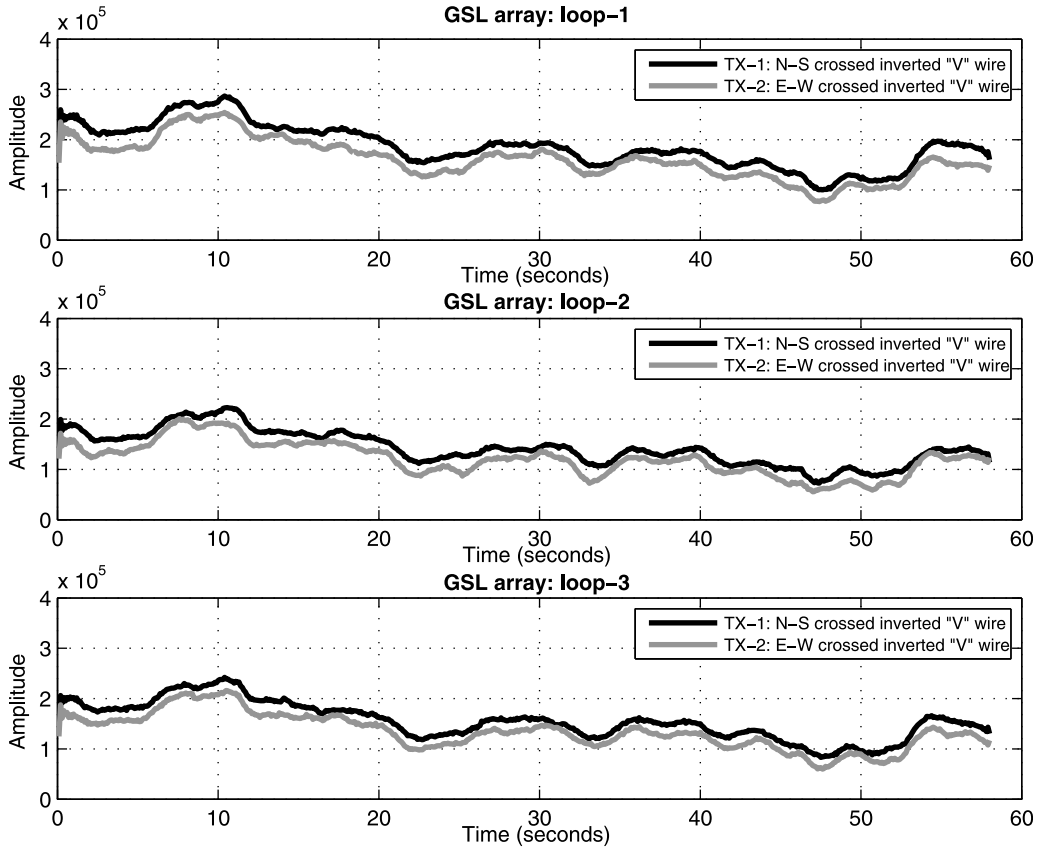

Figure 15. Amplitude patterns (in linear units) observed for a period of approximately 60 s at 1346:00 UT on 29 January 2009 on the three loops comprising the GSL array during a 2 × 8 HF-MIMO measurement campaign conducted between Durham and Bruntingthorpe. Two CW signals (offset from each other by 10 Hz) were transmitted from Durham using the crossed inverted "V" wire antenna array.

that decorrelation between the various antenna elements is achieved at a single location thereby significantly reducing the amounts of physical space required to deploy the HF-MIMO system.

[34] In addition to developing other compact receiving antenna arrays in the future, more emphasis will be placed on the design and investigation of colocated, heterogeneous transmitting antenna arrays. In order to derive a better understanding of the decorrelation behavior, the various antennas that have been utilized in the experiments will be modeled using the numerical electromagnetic code (NEC).

[35] **Acknowledgments.** The authors are grateful to the EPSRC for their financial support of this work. They would also like to thank the UK Solar System Data Centre for provision of data from the Chilton ionosonde.

References

Erhel, Y., D. Lemur, L. Bertel, and F. Marie (2004), HF radio direction finding operating on a heterogeneous array: Principles and experimental validation, *Radio Sci.*, *39*, RS1003, doi:10.1029/2002RS002860.

Erhel, Y. M., C. Perrine, D. Lemur, and A. Bourdillon (2005), Image transmission through ionospheric channel, *Electron. Lett.*, *41*(2), 80–82.

Feeney, S. M., S. Salous, E. M. Warrington, S. D. Gunashekar, N. M. Abbasi, L. Bertel, D. Lemur, and M. Oger (2009), Compact HF antennas for MIMO applications, paper presented at 11th International Conference on Ionospheric Systems and Techniques (IRST 2009), Inst. of Eng. and Technol., Edinburgh, U. K.

Foschini, G. J. (1996), Layered space-time architecture for wireless communication in a fading environment when using multi-element antennas, *Bell Lab. Tech. J.*, *1*(2), 41–59.

Foschini, G. J., and M. J. Gans (1998), On limits of wireless communications in a fading environment when using multiple antennas, *Wirel. Pers. Commun.*, *6*(3), 311–335.

Gething, P. J. D. (1991), *Radio Direction Finding and Superresolution*, 2nd ed., pp. 3–6, Peter Peregrinus, London.

Gunashekar, S. D., E. M. Warrington, S. Salous, S. M. Feeney, H. Zhang, N. M. Abbasi, L. Bertel, D. Lemur, and M. Oger (2008), Early results of experiments to investigate the feasibility of employing MIMO techniques in the HF band, paper presented at Loughborough Antennas and Propagation Conference 2008 (LAPC 2008), Comput. Simul. Technol., Loughborough, U. K.

Gunashekar, S. D., et al. (2009a), Utilization of antenna arrays in HF systems, *Ann. Geophys.*, *52*(3/4), 323–338.

Gunashekar, S. D., E. M. Warrington, S. Salous, S. M. Feeney, N. M. Abbasi, L. Bertel, D. Lemur, and M. Oger (2009b), Investigations into the feasibility of MIMO techniques within the HF band: Preliminary results, *Radio Sci.*, *44*, RS0A19, doi:10.1029/2008RS004075.

Lim, H. M., C. C. Constantinou, and T. N. Arvanitis (2007), On the ensemble average capacity of multiple-input multiple-output channels in outdoor line-of-sight multipath urban environments, *Radio Sci.*, *42*, RS1006, doi:10.1029/2005RS003406.

Loyka, S. L. (2001), Channel capacity of MIMO architecture using the exponential correlation matrix, *IEEE Commun. Lett.*, *5*(9), 369–371.

Marie, F., Y. Erhel, L. Bertel, and D. Lemur (2000), Design of a HF compact direction finding system based on colocated antennas, in *Proceedings of Eighth International Conference on HF Radio Systems and Techniques*, *IEE Conf. Publ.*, *474*, 127–131.

Massie, A., W. Martinsen, D. Taylor, M. Chamalaun, and J. Sorensen (2004), GISELLE-DF using phase data from a ground symmetric loop, paper presented at Fifth Symposium on Radiolocation and Direction Finding, Southwest Res. Inst., San Antonio, Tex.

Mtumbuka, M. C., W. Q. Malik, C. J. Stevens, and D. J. Edwards (2005), A tri-polarized ultra-wideband MIMO system, paper presented at IEEE/Sarnoff Symposium on Advances in Wired and Wireless Communication, Inst. of Electr. and Electron. Eng., Princeton, N. J.

Oger, M., F. Marie, D. Lemur, G. Le Bouter, Y. Erhel, and L. Bertel (2006), A method to calibrate HF receiving antenna arrays, paper presented at 10th International Conference on Ionospheric Radio Systems and Techniques (IRST 2006), Inst. of Eng. and Technol., London.

Perrine, C., Y. Erhel, D. Lemur, L. Bertel, and A. Bourdillon (2004), A way to increase the bit rate in ionospheric radio links, *Ann. Geophys., 47*(2/3), suppl., 1145–1160.

Razavi-Ghods, N., and S. Salous (2009), Wideband MIMO channel characterization in TV studios and inside buildings in the 2.2–2.5 GHz frequency band, *Radio Sci.*, *44*, RS5015, doi:10.1029/2008RS004095.

Shiu, D., G. J. Foschini, M. J. Gans, and J. M. Kahn (2000), Fading correlation and its effect on the capacity of multielement antenna systems, *IEEE Trans. Commun.*, *48*(3), 502–513.

Waldschmidt, C., J. v. Hagen, and W. Wiesbeck (2002), Influence and modelling of mutual coupling in MIMO and diversity systems, *IEEE Antennas Propag. Soc. Int. Symp.*, *3*, 190–193.

Wallace, J. W., and M. A. Jensen (2002), Modeling the indoor MIMO wireless channel, *IEEE Trans. Antennas Propag.*, *50*(5), 591–599.

Warrington, E. M., S. D. Gunashekar, S. Salous, S. M. Feeney, N. M.Abbasi, L. Bertel, D. Lemur, and M. Oger (2008), Investigations into the feasibility of MIMO techniques within the HF band: Preliminary results, paper presented at 12th International Ionospheric Effects Symposium (IES 2008), Off. of Nav. Res., Alexandria, Va.

N. M. Abbasi, S. D. Gunashekar, and E. M. Warrington, Radio Systems Research Group, Department of Engineering, University of Leicester, Leicester LE1 7RH, UK. (emw@leicester.ac.uk)

S. M. Feeney and S. Salous, Centre for Communication Systems, School of Engineering, University of Durham, Durham DH1 3LE, UK.